EMI Filter Integration for GaN Power Module Using Air-Cured Magnetic Composite

Niu Jia
Min H. Kao Department of Electrical Engineering and Computer Science
The University of Tennessee
Knoxville, United States
njia@vols.utk.edu

Leon M. Tolbert
Min H. Kao Department of Electrical Engineering and Computer Science
The University of Tennessee
Knoxville, United States
tolbert@utk.edu

Han (Helen) Cui
Min H. Kao Department of Electrical Engineering and Computer Science
The University of Tennessee
Knoxville, United States
helencui@utk.edu

2023 IEEE Energy Conversion Congress and Exposition (ECCE) | 979-8-3503-1644-5/23/$31.00 ©2023 IEEE | DOI: 10.1109/ECCE53617.2023.10362742

***Abstract*— Severe electromagnetic interference (EMI) issues in wide-bandgap (WBG) power electronics systems result in larger filter sizes to attenuate noise, which compromises the high power density brought by WBG devices. To mitigate the high-frequency EMI noises of WBG systems, integrating a common-mode filter inside the power module is an effective way of managing parasitics in the noise propagation paths and thereby improving the filter performance. However, the magnetic core of a common-mode choke (CMC) takes up considerable height and weight, which lowers the power density of a module. In this paper, an air-cured and module-compatible manufacturing methodology is developed using permalloy-epoxy magnetic composites for the integrated CMC inside a GaN power module.**

The magnetic composite is mixed into a paste texture and can conveniently mold the power module to form the CMC, improving the space utilization and power density of the whole module. This also offers a potential magnetic integration solution for other WBG power modules or circuits. One of the composites has a real part of the complex permeability of 13.5 under high frequency with low core-loss density. A 3-D finite-element model is built to predict the inductance of the over-molded CMC cured with the designed magnetic composite. The manufacturing process of the over-molded CMC is explained and the impact of the magnetic material on the power module parasitics is analyzed. The benefits of the over-molded CMC in EMI reduction and power density improvement are verified by test results, and some suggestions for future optimization are provided.

Keywords*— *Common-Mode Choke, EMI, Epoxy, GaN Power Module Package, Magnetic Composite, Naturally Curable, Permalloy Powder, Potting

I. Introduction

The broad applications of wide-bandgap (WBG) devices in power electronics systems, with increased switching frequency up to megahertz level, contribute to higher efficiency and smaller system size compared to their Si-based counterparts. However, the electromagnetic interference (EMI) noise is aggravated by more switching commutations and higher *dv/dt* [1], which results in a larger EMI filter size for more noise suppression. To fully take advantage of the benefits of WBG devices and maintain high system power density, different methods are explored to mitigate the EMI issues in WBG systems and lessen the design stress on EMI filters.

Regarding the EMI noise source, multiple advanced pulse width modulation methods and improved gate circuits have been developed to reduce the common-mode (CM) current generated by the switches [2]. For mitigation methods targeting the EMI propagation paths, advanced substrates are used in recent power module packaging designs, and methods of eliminating parasitics and couplings existing in the EMI filter and the whole WBG systems are developed and implemented in various research [3]-[7].

Compared to externally-added EMI filters, integrating a common-mode filter in the power module package to manage the parasitics distribution and improve the high-frequency EMI performance is a new attempt in exploring innovation for GaN power modules [8], [9]. However, this filter integration compromises the module's power density due to the height and weight increase brought by the commercial core used in the integrated common-mode choke (CMC). Thus, for the best space utilization in the power module package, there is a need for a flexible and module-compatible magnetic realization with low loss, adequate permeability, and high-frequency stability for the integrated CMC. Various magnetic composites have been developed, but either involve electroplating processes or require high temperature or pressure [10]-[12]. For example, a permalloy-benzocyclobutene magnetic composite designed for high-frequency applications in [12] provides a relative permeability of 26, but it requires a high curing temperature of 250 °C for 30 minutes, which may not be compatible with the GaN power module package since the recommended maximum reflowing temperature for GaN devices is 260 °C for only 30 seconds [13].

In this paper, a manufacturing methodology of permalloy-epoxy magnetic composites is discussed for the CMC integration with the GaN power module. The magnetic composites are module-compatible thanks to their room-temperature and no-pressure manufacturing process, which has the potential for generalized use in other power modules and circuits.

In Section II, magnetic characterization tests of the complex permeability and core-loss density are conducted on the toroid cores cured with the designed magnetic composites. A 3-D finite-element model is constructed in ANSYS Maxwell 3D to correlate the characterization results and predict the inductances

Authorized licensed use limited to: UNIVERSITY OF TENNESSEE LIBRARIES. Downloaded on April 19,2024 at 12:29:54 UTC from IEEE Xplore. Restrictions apply.

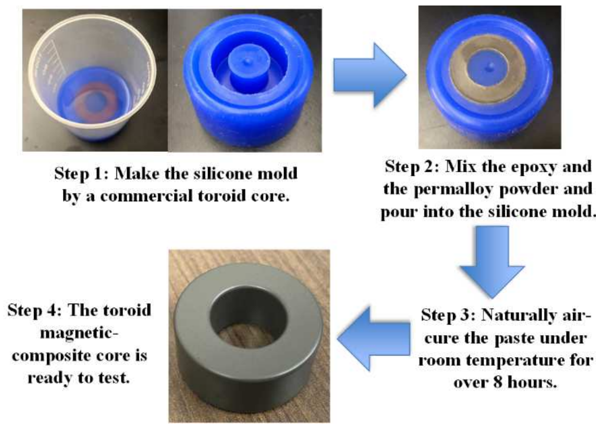

Fig. 1. Toroidal magnetic-composite core manufacturing process.

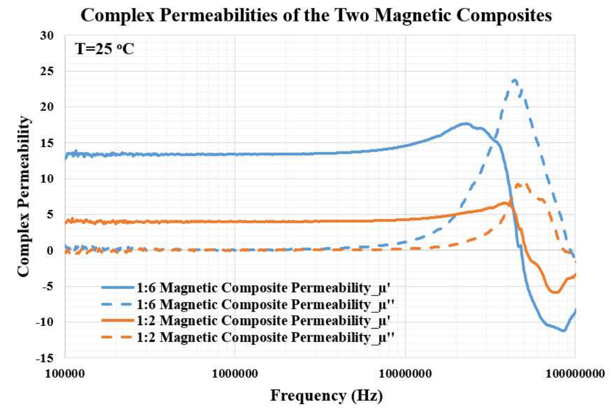

Fig. 2. Complex permeabilities of the designed magnetic composites.

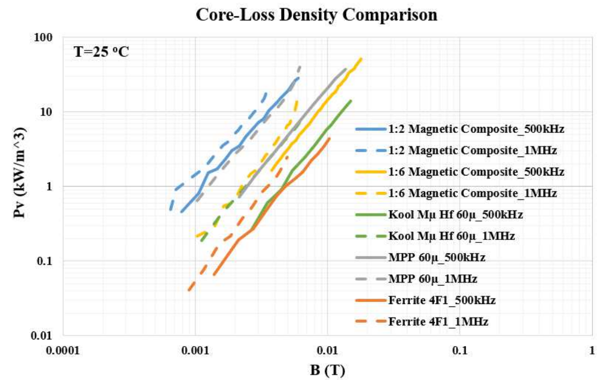

Fig. 3. Core-loss density comparison of the designed magnetic composites and commercial magnetic materials.

of the inductors with magnetic-composite cores cured in various shapes. The magnetic composite with 85.71 weight percent of permalloy powder exhibits a real-part permeability of 13.5 and low core-loss density under high frequency; thus, it is chosen as the magnetic material for the over-molded CMC of a π-type common-mode filter (CMF) as well as the potting material for the GaN power module package.

Section III illustrates the detailed manufacturing process of the over-molded CMC, and the influence of the magnetic material on power module parasitics is discussed through theoretical analysis, simulation, and testing. Design and manufacturing suggestions are provided for future optimization.

In Section IV, three generations of the power modules with different CMCs are compared regarding their power densities and the EMI performance. The power density of the power module with over-molded CMC is almost twice that of power modules with toroid CMC and planar CMC, validating the benefit of the over-molded CMC. The measured CM EMI performance of the power module with the over-molded CMF (comprising both the over-molded CMC and the CM capacitors) verifies the functionality of the over-molded CMC and proves that the increase of the power density brought by the over-molded CMC does not sacrifice the power module's EMI performance. The conclusion and future work are summarized in Section V.

II. Magnetic Composite Manufacturing Process and Characterization

Permalloy powder-325 80 from ESPI Metals with a particle size of less than 44 microns is chosen for its high magnetic permeability and low hysteresis and eddy-current loss. Epoxy resin from PUDUO is selected as the thermoset polymer for its high market availability and good natural curing characteristics. Initially, toroidal magnetic-composite cores are produced for the ease of magnetic characterization. The manufacturing process is introduced, and the complex permeabilities and core-loss densities of two magnetic composites with different weight ratios of epoxy versus magnetic powder are measured in this section.

A. Magnetic Composite Manufacturing Process

The manufacturing process is illustrated in Fig. 1. First, a commercial toroid core [14] is placed in the cup, and silicone gel is poured into the cup and air-cured naturally under room temperature for a duration of over six hours to make the silicone mold. The dimensions of the commercial toroid core can be found in Table. I.

Next, the epoxy liquid is prepared by mixing the epoxy resin and the hardener in a volume ratio of 1:1, which is then mixed with permalloy powder by different weight ratios for magnetic pastes. Subsequently, the magnetic paste is poured into the silicone mold and shaken to eliminate any trapped air voids. Finally, the magnetic paste is naturally air-cured at room temperature for over 8 hours. The completed toroidal magnetic-composite core, with a weight ratio of epoxy to permalloy powder of 1:6, is shown in Fig. 1 Step 4.

TABLE I. Toroid Core Dimensions [14]

Dimensions	Values
Outer Diameter (mm)	25
Inner Diameter (mm)	16
Height (mm)	10

Authorized licensed use limited to: UNIVERSITY OF TENNESSEE LIBRARIES. Downloaded on April 19,2024 at 12:29:54 UTC from IEEE Xplore. Restrictions apply.

Dimensions	Values
l_e (mm)	64.4
A_e (mm^2)	36
V_e (mm^3)	2318.4

(a) (b)

Fig. 4. (a) 11-turn toroidal inductor with 1:6 magnetic composite core; (b) 3-D finite-element model of the 11-turn toroidal inductor.

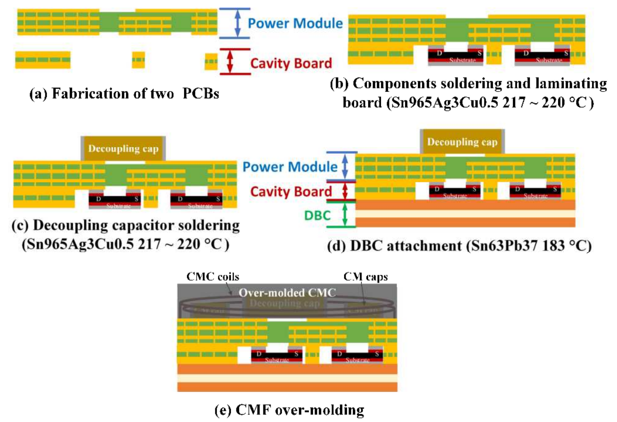

Fig. 5. Fabrication process of the GaN power module with over-molded CMF.

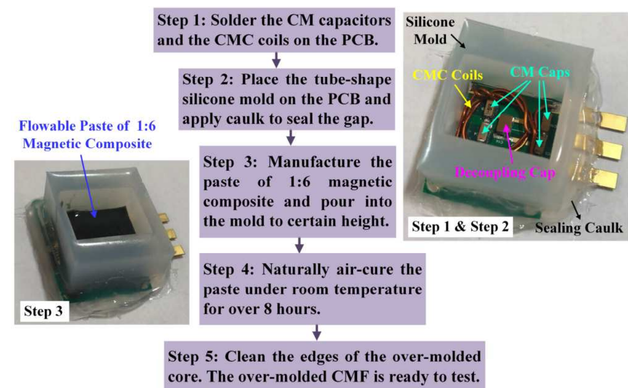

Fig. 6. Flow chart for CMF over-molding on the GaN power module (Fig. 5(e)).

B. *Magnetic Characterization*

Magnetic composites with weight ratios of epoxy versus permalloy powder at 1:2 and 1:6 are produced for comparison purposes, hereinafter referred to as 1:2 magnetic composite and 1:6 magnetic composite, respectively. The curves of complex permeability versus frequency for the two magnetic composites are derived from the inductance measurement method conducted with network analyzer E5061B (5 Hz-3 GHz) from Keysight and shown in Fig. 2. The complex permeability of the 1:2 magnetic composite shows a similar trend to that of the 1:6 magnetic composite but with lower values. 1:6 magnetic composite demonstrates a steady real part μ' of 13.5 up to around 30 MHz, and the high imaginary part μ" beyond 40 MHz provides a high impedance, also contributing to the high-frequency attenuation of the CMC [15].

The core-loss density versus magnetic flux density under 500 kHz and 1 MHz of the two designed magnetic composites, as well as commercial magnetic materials Kool Mμ H*f* 60μ and MPP 60μ from Magnetics Inc., and ferrite 4F1 from Ferrocube, are tested under room temperature using method from [16] and compared in Fig. 3. It can be concluded that among all the materials tested, ferrite 4F1 presents the smallest core-loss density at 500 kHz and 1 MHz, attributing to its high-temperature and high-pressure compressing and sintering manufacturing process. The designed magnetic composites present comparably low core-loss densities which are similar to those of the commercial powder cores. It is worth noting that the commercial powder cores are fabricated with a pressurized process, while the magnetic composites described in this paper involve no pressure during the fabrication. These test results indicate that the designed magnetic composites offer effective solutions for high-frequency magnetic integration with low core loss.

C. *Simulation for Inductance Prediction*

Based on the magnetic characterization results, 1:6 magnetic composite is selected as the magnetic material for the over-molded CMC because of its higher permeability and lower core-loss density. The material properties are input into ANSYS Maxwell 3D to build a 3-D finite-element model of an 11-turn toroidal inductor shown in Fig. 4(b). The simulated inductance value obtained from the model is 2.01 μH, which closely matches the measured inductance of 1.91 μH for the inductor shown in Fig. 4(a), enabling the capability of the model to predict the inductance of the over-molded choke when integrated with the GaN power module.

III. GaN Power Module with Over-Molded Choke

In this section, the module-compatible manufacturing process of the over-molded CMC is explored. The inductance of the CMC is determined by comparing the impedance measurement of the CMF with the simulated results obtained through parameter sweeping in LTspice. The influence of the magnetic material on two power module parasitics is analyzed, and design and manufacturing suggestions are provided for future optimization.

A. *Over-molded Choke Manufacturing Process*

The structure and fabrication process of the GaN power module with a non-over-molded CMC are illustrated in Fig. 5 of [17]. However, in the manufacturing process of the power module with over-molded CMC, due to the irreversibility of the over-molding process, the power module is first tested with

Authorized licensed use limited to: UNIVERSITY OF TENNESSEE LIBRARIES. Downloaded on April 19,2024 at 12:29:54 UTC from IEEE Xplore. Restrictions apply.

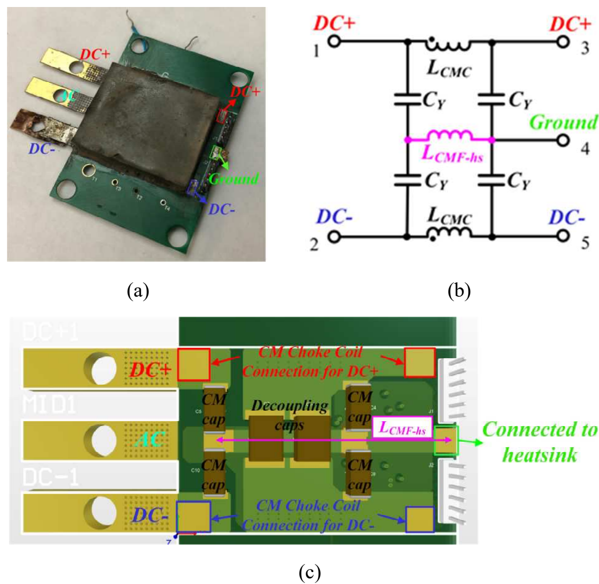

Fig. 7. (a) Prototype of the GaN power module with over-molded CMF, (b) π-type CMF structure. (c) GaN power module PCB top view.

DBC attached before over-molding the CMC to ensure its electrical function. Thus, the fabrication process of the GaN power module is optimized as Fig. 5(a)-(e) show, where Fig. 5(e) is further explained by a flow chart in Fig. 6.

After testing the power module with DBC, the two 3-turn coupled coils of the CMC hand-wound with magnet wires, and four 1-nF CM capacitors are soldered on the printed circuit board (PCB) of the power module. Next, a tube-shaped silicone mold with a height scale that encloses the area of the over-molded choke is placed on the PCB. To prevent magnetic paste leakage, water-proof caulk is applied around the power module to seal the gap between the silicone mold and the PCB. The flowable paste of 1:6 magnetic composite is then made and poured into the mold to a certain height. Finally, the power module is naturally air-cured under room temperature for over 8 hours.

The finished over-molded CMC with a height of 4.5 mm is shown in Fig. 7(a). This approach allows the 1:6 magnetic composite to serve not only as the magnetic material for the high-frequency integrated CMC but also as the potting material of the GaN power module to encapsulate the top side of the PCB.

B. Over-molded Choke Characterization

The characterization procedure for the over-molded structure, in general, is nontrivial since the choke inductor, as well as its peripheral components, are connected and encapsulated, making it difficult to decouple the measurement results from other components and parasitics. The equivalent circuit of the π-type CMF over-molded on the GaN power module is presented in Fig. 7(b). Here, L_{CMC} and C_Y represent the CMC inductance and CM capacitance ($C_Y = 1$ nF). $L_{CMF\text{-}hs}$ is a non-negligible parasitic inductance labeled in Fig. 7(c), caused by the PCB trace that connects the CM capacitors to the heatsink which is assumed to be connected to the ground. Ports 1 to 5, as labeled in Fig. 7(a), can be leveraged as filter impedance-measuring ports. In this case, the impedance of the whole CMF is measured with network analyzer E5061B across a frequency range of 1 MHz to 500 MHz, and an LTspice model is constructed for parameter sweeping to match the impedance measurement and obtain the inductance of the over-molded CMC.

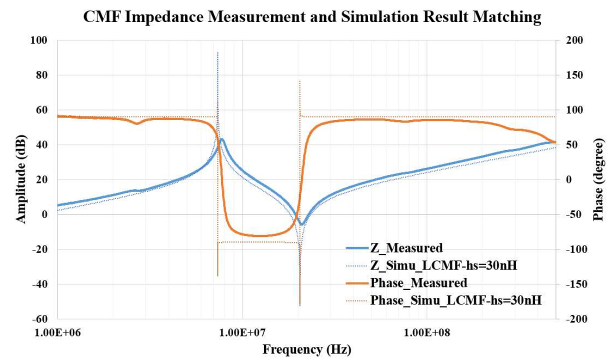

Fig. 8. CMF impedance measurement and simulation result matching.

To simplify the filter structure and facilitate impedance matching, Port 1 is connected with Port 2, and Port 3 is connected with Port 4 and Port 5. The measurement is taken at Port 2 and Port 5. Since the LTspice model does not incorporate resistances, the focus of the impedance matching lies in the resonant frequencies rather than the amplitude. The coupling coefficient K used in the LTspice model is obtained as 0.7 by measuring a coupled inductor with the same coil structure as the over-molded CMC.

According to the parameter sweeping result, $L_{CMC} = 240$ nH is obtained which aligns with the first resonant peak of the measured impedance curve caused by the resonance of the CMC inductance and the CM capacitance. This value is lower than the simulated inductance from ANSYS, mainly due to the limited volume of the magnetic material and the air voids induced by the complex and irregular hand-wound coils of the CMC, which cannot be fully depicted in the simulation model. The value of $L_{CMF\text{-}hs}$ is swept from 10 nH to 30 nH to match the remaining resonant frequency, and it is found that the matching is optimized when $L_{CMF\text{-}hs}$ equals 30 nH.

The results of the impedance measurement and the LTspice model simulation are shown in Fig. 8, where a good match is achieved using the results of parameter sweeping for simulation. It should be noted that if there are multiple sets of parameters that can fit the measurement result, then different structures should be measured and simulated by connecting the five ports in different ways to obtain the most optimized set of parameters.

C. Molding Material's Influence on the Parasitics in the Power Module

One major concern of magnetic integration in the WBG power module package is that the magnetic material may impact the parasitic inductances of the power module and undermine the power module's performance. For instance, the power loop parasitic inductance L_{loop} is a parasitic existing in the power module power loop, which significantly affects the switching performance of the switching devices, making it an essential

Authorized licensed use limited to: UNIVERSITY OF TENNESSEE LIBRARIES. Downloaded on April 19,2024 at 12:29:54 UTC from IEEE Xplore. Restrictions apply.

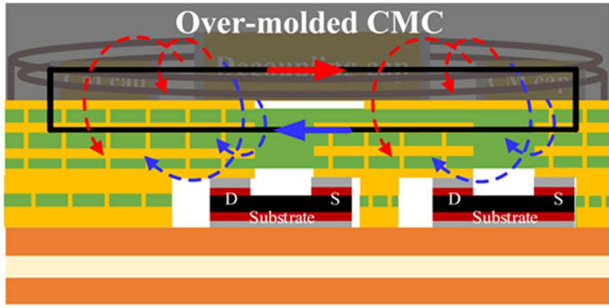

(a)

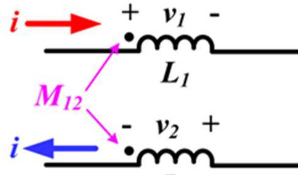

(b)

Fig. 9. (a) magnetic flux cancellation in vertical power loop of the designed GaN power module with over-molded CMC, (b) equivalent circuit.

factor to evaluate a power module design. A large L_{loop} leads to higher voltage overshoot on the device and worsens the EMI performance. Therefore, minimizing L_{loop} is a key design objective for power modules [18], while including magnetic material in the package may cause the opposite effect.

This requires some special considerations in the design phase of the power module package. Forming a vertical power loop by the switches and the decoupling capacitors is a popular design method used for power module layout, which utilizes magnetic flux cancellation to reduce the power loop parasitic inductance. While the size of the lateral power loop is usually restricted by the sizes of the components and the required creepage distance, and cannot be minimized, the vertical power loop can be seen as two horizontal conductors placed closely in parallel because of the short length of the vertical traces in a PCB.

The principle of magnetic flux cancellation is depicted in Fig. 9(a). Because the currents flowing through the two conductors are in opposite directions, the two types of magnetic flux existing in their outer area are also in opposite directions, realizing the magnetic flux cancellation and effectively reducing the parasitic inductance [19]. The equivalent circuit is shown in Fig. 9(b). Compared to a lateral design, the vertical power loop parasitic inductance L_{loop} is reduced by 2*M_{12} as (1) calculates

$$L_{loop} = L_1 + L_2 - 2M_{12} \tag{1}$$

In the designed GaN power module with over-molded CMC, the magnetic paste only covers the area where the magnetic flux cancels, while the center area inside the vertical loop where the magnetic fields superimpose is not affected. Therefore, the loop inductance is expected to remain similar to that without magnetic molding.

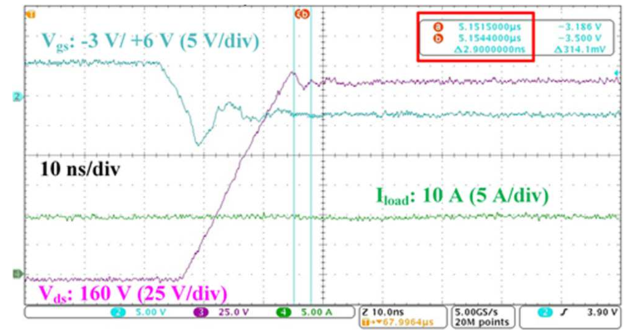

(a)

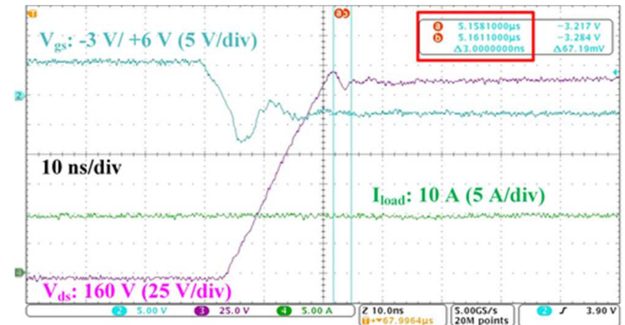

(b)

Fig. 10. DPT results under 160 V/10 A for (a) power module without over-molded CMF, (b) power module with over-molded CMF.

The assumption above is validated by both simulations and measurements. Models of the GaN power modules with and without over-molded CMC are constructed in ANSYS Q3D Extractor. The power loop parasitic inductance of the power module without over-molded CMC is extracted as 1.098 nH while that of the power module with the over-molded CMC is 1.165 nH. Thus, there is no obvious difference between the power loop parasitic inductances extracted under both conditions.

Double-pulse tests (DPTs) are conducted to verify the simulations. Power loop parasitic inductance can be calculated by (2) through the DPT, where T is the ringing time period, measured by the time interval of the first and second oscillation peaks of the turn-off waveform; C_{oss} is the output capacitance of the device under test, which is 261 pF at 160 V; C_{para} is a 1.5-pF parasitic capacitance caused by PCB traces; and C_{probe} is a 1.8-pF parasitic capacitance caused by passive probe [17].

$$L_{loop} = \frac{T^2}{4\pi^2(C_{oss}+C_{para}+C_{probe})} \tag{2}$$

DPTs are conducted under 160 V/10 A for both power modules with and without over-molded CMC, as shown in Fig. 10, to compare the impact of the magnetic material on the power loop parasitic inductance. For the power module without over-molded CMC, the time period T is tested to be 2.9 ns, resulting in a calculated L_{loop} of 0.806 nH. And for the power module with over-molded CMC, the time period is tested as

Authorized licensed use limited to: UNIVERSITY OF TENNESSEE LIBRARIES. Downloaded on April 19,2024 at 12:29:54 UTC from IEEE Xplore. Restrictions apply.

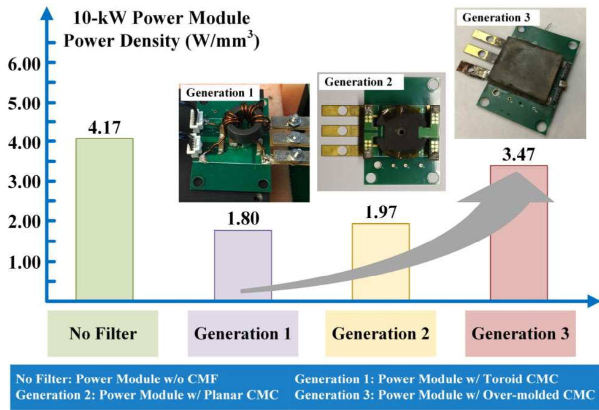

Fig. 11. Roadmap for power densities of power module with different CMCs [8], [9].

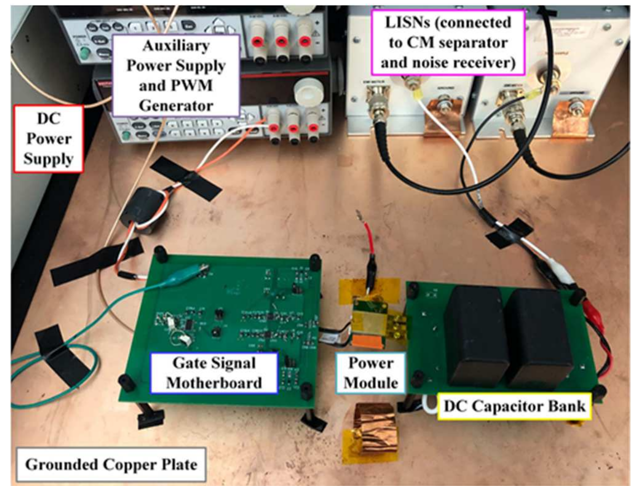

Fig. 12. CM EMI test setup.

3.0 ns, so L_{loop} is calculated as 0.863 nH. The difference in the loop inductances between the two cases is relatively minor, with a difference percentage of 7.07%, indicating that the magnetic-composite core does not have a significant influence on the parasitic inductance in the vertical power loop. Besides, the permeability of the 1:6 magnetic composite is only 13.5 under ideal conditions. In the real over-molded CMC, it could potentially be even lower due to the presence of air voids caused by the complex coil structure and the limited volume of magnetic material, which is further reduced by the inclusion of capacitors and coils within the magnetic-composite core.

However, the presence of the magnetic material in the over-molded CMC does have an appreciable impact on parasitic inductance from exposed PCB traces, such as the CMF-to-heatsink parasitic inductance $L_{CMF\text{-}hs}$ caused by the PCB trace that connects the CM capacitors and the grounded heatsink as Fig. 7(c) shows. The parameter sweeping result of $L_{CMF\text{-}hs}$ is 30 nH, which reveals a noticeable increase of $L_{CMF\text{-}hs}$ measured with the over-molded CMC, compared to the value of 9.6 nH extracted by ANSYS Q3D extractor without the over-molded CMC [8]. This increase may undermine the benefit of the CMF integration, as a small $L_{CMF\text{-}hs}$ is desired for optimal EMI performance. The reason is that this PCB trace is placed laterally under and directly contacts the magnetic material with a long return path. As a result, it is more susceptible to the influence of the magnetic material, leading to the observed higher value of $L_{CMF\text{-}hs}$ when the over-molded CMC is present. The behavior comparison of the two parasitic inductances inspires some design considerations for the WBG power module with magnetic integration as illustrated in Section III-D.

D. Design and Manufacturing Considerations

Based on previous analysis, several design considerations are given below for future optimization of the power module design and over-molded CMC manufacturing. For the power module design, vertical loops are preferred when integrating magnetic materials, which help to mitigate the influence of the magnetic material on loop parasitic inductance. For lateral loops that may be affected by the integrated magnetic material, additional design techniques such as shielding layers should be applied to the design [20].

For over-molded CMC design and manufacturing, improving the design of CMC coils to increase the coupling coefficient and minimize the complexity of the coil structure is the next step. The current CMC coils are made by hand-wound magnet wires, and the two sides of windings are twisted together to increase the coupling coefficient, introducing air voids within the magnetic-composite core and leading to reduced inductance. Curing the over-molded CMC in a vacuum chamber can help eliminate or reduce the presence of air voids within the magnetic-composite core, ensuring better performance and higher inductance. These improvement measures will be evaluated in subsequent work.

IV. Experimental Verification of Over-Molded Choke

In this section, the power densities of power modules with different CMCs are compared to verify the benefit of the over-molded CMC. The function of the over-molded CMC is validated by measuring the CM EMI spectra of the power module with over-molded CMC and comparing them with those of the power module without CMF and with planar CMC. The results prove that the over-molded CMC realizes the increase of the power density while not sacrificing the EMI filtering ability.

A. Power Density Comparison

The roadmap for the power densities of the 10-kW power module with developing CMCs is shown in Fig. 11, where three generations are compared with the power module without CMF, and a clear increase of the power density has been realized by the power module with over-molded CMC. The dimension of the power module is 27 mm in length and 18 mm in width. The height from DBC to PCB is 1.434 mm, which is the same for all three generations. However, the overall height of each generation differs due to the components above the power module PCB. The GaN power module without CMF is 4.934 mm in height because 3.5-mm high decoupling capacitors are used. The heights for the toroid CMC and the planar CMC are 6.5 mm and 5.5 mm so the overall heights of Generation 1 and 2 are 11.434 mm and 10.434 mm, respectively.

Notably, for the power module with over-molded CMC, the decoupling capacitors and the CM capacitors are molded inside

Authorized licensed use limited to: UNIVERSITY OF TENNESSEE LIBRARIES. Downloaded on April 19,2024 at 12:29:54 UTC from IEEE Xplore. Restrictions apply.

the 1:6 magnetic-composite core, so only the 4.5-mm height of the over-molded CMC is added to the total height of the power module, while the capacitors remain within the core. The over-molded CMC achieves a better magnetic design and optimizes the space utilization within the power module, resulting in only a 1-mm increase in height compared to the power module without CMF. The power density is nearly doubled compared to power modules employing toroid CMC and planar CMC, primarily due to the significant reduction in overall height, as depicted in Fig. 11.

B. EMI Test Results

In this paper, the frequency range of the radiated EMI is focused on due to the increasing high-frequency noise generated by WBG devices. The CM conduction current as the radiation source is measured by a pair of line impedance stabilization networks (LISNs) as an indicator of the radiated EMI noise [8]. The CM EMI test setup is shown in Fig. 12. The DC voltage is applied to the half-bridge power module without loads. The CM conduction current is generated by continuous hard-switching operations of the half-bridge under 70 V/80 kHz. The spectra of the CM voltages, obtained by LISNs' measurement, are shown in Fig. 13. The CM EMI noise of the following three cases is compared under the same test setup and conditions: 1) the power module without CMF, 2) the power module with planar CMC, and 3) the power module with over-molded CMC.

As shown in Fig. 13, the power module with over-molded CMC exhibits good EMI noise attenuation across the entire frequency range of 30-100 MHz compared to the power module without CMF, showing that the over-molded CMC serves its function as an EMI noise filter. And compared to that of the power module with planar CMC, the CM EMI spectra of the power module with over-molded CMC have similar but shifted resonances. This disparity is caused by the different inductances and coupling coefficients of the two generations of the CMCs. For future work, the optimization of over-molded CMC manufacturing is anticipated to increase the inductance, thereby shifting the resonance peak to a lower frequency range, thus minimizing its impact on the high-frequency performance of the CMF.

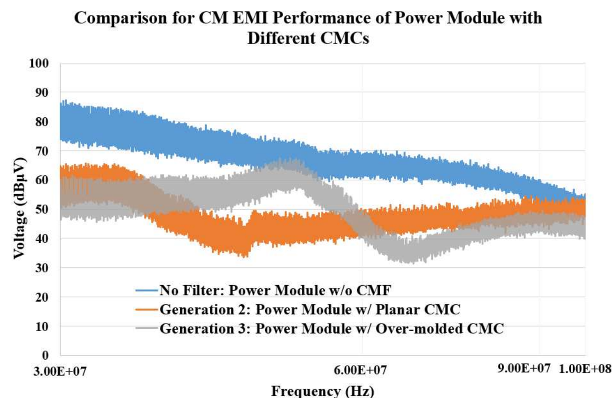

Fig. 13. Comparison of CM EMI spectra for the power module with different CMCs from 30 MHz to 100 MHz [8].

V. CONCLUSIONS

This paper presented an air-cured manufacturing methodology of permalloy-epoxy magnetic composites, aimed at increasing the overall power density of GaN power module packages with high-frequency integrated CMC. Two types of magnetic composites, with epoxy and permalloy powder weight ratios of 1:2 and 1:6, were fabricated and compared, finding that under room temperature 1:6 magnetic composite has a complex permeability of 13.5 for the real part, good high-frequency stability and low core-loss density, making it a good choice of the CMC's core material.

The power module with over-molded CMC made by 1:6 magnetic composite was fabricated with CMC coils, decoupling capacitors, and CM capacitors molded inside the magnetic-composite core to form an integrated π-type CMF. The manufacturing process of the over-molded CMC was explained, and the influence of the magnetic material on two power module parasitics, namely power loop parasitic inductance and the CMF-to-heatsink parasitic inductance, was discussed through theoretical analysis, simulation and testing. Based on these findings, suggestions on power module design and over-molded CMC manufacturing were provided for future improvement.

The vertical loop can effectively mitigate the increase of the loop parasitic inductance, underscoring the importance of realizing a vertical power loop configuration for power modules. CM EMI tests were conducted for power modules without filter, with planar CMC, and with over-molded CMC, confirming the functionality of the over-molded CMC in reducing CM EMI noise. The power density of the GaN power module with over-molded CMC was calculated and compared with those of the power module with other CMCs, validating the high power density brought by the magnetic integration with the designed magnetic composite.

In the future, this easy-to-implement air-cured manufacturing methodology holds potential as a magnetic integration solution for other WBG power modules or circuits while maintaining vertical power loops. It would particularly benefit applications that are more sensitive to the power loop parasitic inductance, such as point of load module, enabling high integration and efficiency simultaneously.

REFERENCES

[1] J. Yao, Y. Lai, Z. Ma and S. Wang, "Investigation of Noise Spectrum and Radiated EMI in High Switching Frequency Flyback Converters," *2021 IEEE Applied Power Electronics Conference and Exposition (APEC)*, Phoenix, AZ, USA, 2021, pp. 2265-2270, doi: 10.1109/APEC42165.2021.9487418.

[2] Z. Zhang, Y. Hu, X. Chen, G. W. Jewell and H. Li, "A Review on Conductive Common-Mode EMI Suppression Methods in Inverter Fed Motor Drives," in *IEEE Access*, vol. 9, pp. 18345-18360, 2021, doi: 10.1109/ACCESS.2021.3054514.

[3] A. I. Emon, Z. Yuan, A. B. Mirza, A. Deshpande, M. U. Hassan and F. Luo, "1200 V/650 V/160 A SiC+Si IGBT 3L Hybrid T-Type NPC Power Module With Enhanced EMI Shielding," in *IEEE Transactions on Power Electronics*, vol. 36, no. 12, pp. 13660-13673, Dec. 2021, doi: 10.1109/TPEL.2021.3089578.

[4] X. Li et al., "EMI Mitigation with Stacking DBC Substrate for High Voltage Power Module," *2022 IEEE Energy Conversion Congress and Exposition (ECCE)*, Detroit, MI, USA, 2022, pp. 1-7, doi: 10.1109/ECCE50734.2022.9947391.

Authorized licensed use limited to: UNIVERSITY OF TENNESSEE LIBRARIES. Downloaded on April 19,2024 at 12:29:54 UTC from IEEE Xplore. Restrictions apply.

[5] J.-W. Shin, C.-M. Wang and E. M. Dede, “Power Semiconductor Module With Low-Permittivity Material to Reduce Common-Mode Electromagnetic Interference,” in *IEEE Transactions on Power Electronics*, vol. 33, no. 12, pp. 10027-10031, Dec. 2018, doi: 10.1109/TPEL.2018.2828041.

[6] J. Yao, Y. Li, S. Wang, X. Huang and X. Lyu, “Modeling and Reduction of Radiated EMI in a GaN IC-Based Active Clamp Flyback Adapter,” in *IEEE Transactions on Power Electronics*, vol. 36, no. 5, pp. 5440-5449, May 2021, doi: 10.1109/TPEL.2020.3032644.

[7] R. Phukan et al., “Characterization and Mitigation of Conducted Emissions in a SiC Based Three-Level T-Type Motor Drive for Aircraft Propulsion,” in *IEEE Transactions on Industry Applications*, vol. 59, no. 3, pp. 3400-3412, May-June 2023, doi: 10.1109/TIA.2023.3252521.

[8] N. Jia, X. Tian, L. Xue, H. Bai, L. M. Tolbert and H. Cui, “Integrated Common-Mode Filter for GaN Power Module With Improved High-Frequency EMI Performance,” in *IEEE Transactions on Power Electronics*, vol. 38, no. 6, pp. 6897-6901, June 2023, doi: 10.1109/TPEL.2023.3248092.

[9] N. Jia, X. Tian, L. Xue, H. Bai, L. M. Tolbert and H. Cui, “In-Package Common-Mode Filter for GaN Power Module with Improved Radiated EMI Performance,” *2022 IEEE Applied Power Electronics Conference and Exposition (APEC)*, Houston, TX, USA, 2022, pp. 974-979, doi: 10.1109/APEC43599.2022.9773764.

[10] Yun-Tien Chen et al., “Electrical and temperature characterization of flexible planar inductor,” *2012 7th International Microsystems, Packaging, Assembly and Circuits Technology Conference (IMPACT)*, Taipei, 2012, pp. 363-366 , doi: 10.1109/IMPACT.2012.6420267.

[11] C. Ding, K. D. T. Ngo and G. -Q. Lu, “A Soft Magnetic Moldable Composite With Tri-Modal Size Distribution for Power Electronics Applications,” in *IEEE Transactions on Magnetics*, vol. 57, no. 3, pp. 1-6, March 2021, , doi: 10.1109/TMAG.2021.3053176.

[12] Y. Yan, W. Sun, S. Gao, T. Ge, K. D. T. Ngo and G. -Q. Lu, “Design, Fabrication, and Characterization of a Low-Temperature Curable Magnetic Composite for Power Electronics Integration,” in *IEEE Transactions on Magnetics*, vol. 54, no. 1, pp. 1-6, Jan. 2018, , doi: 10.1109/TMAG.2017.2757020.

[13] GaN Systems, *GS-065-060-3-B 650 V E-mode GaN transistor Datasheet*. [Online]. Availble: https://gansystems.com/wp-content/uploads/2022/03/GS-065-060-3-B-DS-Rev-220131.pdf

[14] Vacuumschmelze, *Specification for Soft Magnetic Cores*. [Online]. Availble: https://vacuumschmelze.com/03_Documents/Datasheets%20-%20Drawings/Cores/L2025-W375.pdf

[15] R. Ren, Z. Dong, B. Liu and F. Wang, “Impedance-based Common-mode Inductor Design Approach Considering Frequency-dependent and Imaginary Permeability,” *2020 IEEE Applied Power Electronics Conference and Exposition (APEC)*, New Orleans, LA, USA, 2020, pp. 2680-2686, doi: 10.1109/APEC39645.2020.9124471.

[16] M. Mu, Q. Li, D. J. Gilham, F. C. Lee and K. D. T. Ngo, “New Core Loss Measurement Method for High-Frequency Magnetic Materials,” in *IEEE Transactions on Power Electronics*, vol. 29, no. 8, pp. 4374-4381, Aug. 2014, doi: 10.1109/TPEL.2013.2286830.

[17] X. Tian et al., “An Embedded GaN Power Module with Double-Sided Cooling and High-Density Integration,” *2022 IEEE Energy Conversion Congress and Exposition (ECCE)*, Detroit, MI, USA, 2022, pp. 1-7, doi: 10.1109/ECCE50734.2022.9947786.

[18] I. Josifović, J. Popović-Gerber and J. A. Ferreira, “Improving SiC JFET Switching Behavior Under Influence of Circuit Parasitics,” in *IEEE Transactions on Power Electronics*, vol. 27, no. 8, pp. 3843-3854, Aug. 2012, doi: 10.1109/TPEL.2012.2185951.

[19] S. -S. Min, C. -H. Eom, Y. -S. Jang and R. -Y. Kim, “Three-Dimensional Lattice Structure to Reduce Parasitic Inductance for WBG Power Semiconductor-Based Converters”, *Electronics*, vol. 12, pp. 1779, Apr. 2023, doi: 10.3390/electronics12081779.

[20] S. Ji, D. Reusch and F. C. Lee, “High frequency high power density 3D integrated Gallium Nitride based point of load module,” *2012 IEEE Energy Conversion Congress and Exposition (ECCE)*, Raleigh, NC, USA, 2012, pp. 4267-4273, doi: 10.1109/ECCE.2012.6342242.

Authorized licensed use limited to: UNIVERSITY OF TENNESSEE LIBRARIES. Downloaded on April 19,2024 at 12:29:54 UTC from IEEE Xplore. Restrictions apply.